Published in final edited form as:
J Biol Chem. 2007 February 9; 282(6): 4210–4217. doi:10.1074/jbc.M606300200.

Hormonal Regulation of Nuclear Permeability[*,◆]

Elizabeth M. O'Brien, **Dawidson A. Gomes**, **Sona Sehgal**, and **Michael H. Nathanson**[1]
Department of Medicine, Yale University School of Medicine, New Haven, Connecticut 06520-8019

Abstract

Transport into the nucleus is critical for regulation of gene transcription and other intranuclear events. Passage of molecules into the nucleus depends in part upon their size and the presence of appropriate targeting sequences. However, little is known about the effects of hormones or their second messengers on transport across the nuclear envelope. We used localized, two-photon activation of a photoactivatable green fluorescent protein to investigate whether hormones, via their second messengers, could alter nuclear permeability. Vasopressin other hormones that increase cytosolic Ca^{2+} and activate protein kinase C increased permeability across the nuclear membrane of SKHep1 liver cells in a rapid unidirectional manner. An increase in cytosolic Ca^{2+} was both necessary and sufficient for this process. Furthermore, localized photorelease of caged Ca^{2+} near the nuclear envelope resulted in a local increase in nuclear permeability. Neither activation nor inhibition of protein kinase C affected nuclear permeability. These findings provide evidence that hormones linking to certain G protein-coupled receptors increase nuclear permeability via cytosolic Ca^{2+}. Short term regulation of nuclear permeability may provide a novel mechanism by which such hormones permit transcription factors and other regulatory molecules to enter the nucleus, thereby regulating gene transcription in target cells.

The nuclear envelope represents a structural and functional barrier to passage between the nucleus and the cytosol. Regulation of the permeability of this barrier is one potential mechanism to control access to the nucleus for proteins that affect nuclear function, including transcription factors and various kinases and phosphatases. Nucleocytosolic passage generally occurs through the nuclear pore complex (1,2), a 125-MDa membrane-spanning protein complex consisting of eight ion channels and a large central passage (3). Movement of molecules through the nuclear pore is restricted on the basis of size and the presence or absence of appropriate localization sequences. Studies using electron scanning microscopy (4), fluorescence recovery after photo-bleaching techniques (5), and microinjection of fluorescently labeled dextrans (6) have shown that molecules up to 40–60 kDa in size can cross the nuclear envelope without a signaling sequence. Proteins less than 4–10 kDa in size freely pass from cytosol to nucleus (6–8), while intermediate sized proteins (19–40 kDa) do not need a targeting sequence to cross the nuclear pore, but the permeability of the pore to such molecules may be modulated (6-8). One factor that appears to regulate the permeability of the nuclear pore to proteins in this intermediate size range is the amount of Ca^{2+} within the nuclear envelope (6-9), although there is now conflicting evidence about this (5). Little is known about the role of cytosolic factors such as second messengers in the regulation of nuclear pore permeability.

[*]This work was supported by National Institutes of Health Grants DK45710, DK57751, DK07356, and DK34989. The costs of publication of this article were defrayed in part by the payment of page charges. This article must therefore be hereby marked "*advertisement*" in accordance with 18 U.S.C. Section 1734 solely to indicate this fact.

◆This article was selected as a Paper of the Week.

1 To whom correspondence should be addressed: Section of Digestive Diseases, Yale University School of Medicine, 1 Gilbert St., Rm. TAC S241D, New Haven, CT 06520-8019. Tel.: 203-785-7312; Fax: 203-785-4306; michael.nathanson@yale.edu..

The spatial pattern of second messenger signals is important for how these signals regulate cell function. This has been demonstrated through a number of examples for Ca^{2+} signals (10), and evidence suggests that the spatial pattern of protein kinase C (PKC)[2] and cAMP similarly is important for the specificity of their effects. For example, Ca^{2+} signals in the cytosol and nucleus have different effects on gene transcription. Ca^{2+} signals in the cytosol activate transcription factors such as SRE (11), whereas Ca^{2+} signals in the nucleus instead activate CRE (11) and Elk-1 (12). Moreover, Ca^{2+} increases within the cytosol can have differing effects depending on the region of cytosol where the increase occurs. Presynaptic increases in Ca^{2+} in neurons (13,14) or apical increases in Ca^{2+} in polarized epithelia (15) can trigger exocytosis, while perimitochondrial increases in Ca^{2+} can induce apoptosis (16). Activation of certain isoforms of PKC is associated with their translocation to the plasma membrane (17,18), and activation of intranuclear PKC may similarly require translocation to the nuclear envelope (19). Finally, subplasmalemmal increases in cAMP are associated with glucagon-induced insulin secretion (20). Based on these examples, it might be expected that local increases in second messengers in the region of the nuclear pore could regulate pore permeability. Calmodulin may interact with the nuclear pore (21) so one specific hypothesis is that cytosolic Ca^{2+} could modulate pore permeability. Therefore we investigated the effects on nuclear membrane permeability of hormones that act through G_q to increase cytosolic Ca^{2+}.

EXPERIMENTAL PROCEDURES

Materials, Reagents, and Cell Lines

The SKHep1 liver cell line (ATCC, Manassas, VA) was used for all experiments. Cells were grown at 37 °C with 5% CO_2:95% O_2 in Dulbecco's modified Eagle's medium (Invitrogen) supplemented with 1% penicillin-streptomycin antibiotics (Invitrogen) and 5% heat-inactivated fetal bovine serum (Invitrogen). Cells were grown on glass coverslips overnight before transfection, when the medium was changed to one identical but lacking antibiotics. Opti-MEM (Invitrogen) and Lipofectamine 2000 (Invitrogen) were used during transfections. A photo-activatable green fluorescent protein (PA-GFP (22)) construct was a kind gift from Dr. L. Cooley (Yale University). A DsRed construct targeted to the cytosol with a nuclear exclusion sequence (NES) was obtained from Clontech (Mountain View, CA). Vasopressin (AVP), phorbol 12,13-dibutyrate (PDBu), thapsigargin, angiotensin, phenylpherine, ATP, a myristolated PKC inhibitor, prazosin, suramin, [Sar^1, Val^5, Ala^8]angiotensin II acetate, and [deaminopen ,*O*-Me-Tyr^2,Arg^8]vasopressin were purchased from Invitrogen. The acetoxymethyl (AM) ester forms of BAPTA, Fura Red, and DM-nitrophen (caged calcium) also were from Invitrogen. Dithiothreitol was purchased from American Bio-analytical (Natick, Massachusetts).

Transfection and Perfusion

Cells were grown on glass coverslips for 24–48 h to reach 60% confluence and then transferred to Dulbecco's modified Eagle's medium containing 5% fetal bovine serum. Cells were co-transfected with PAGFP plus DsRed-NES using Lipofectamine 2000 according to the manufacturer's instructions. Transfected cells were incubated for a further 24 h before use.

Fluorescence Imaging

For imaging studies, cells were transferred to HEPES buffer, pH 7.4, and placed in a custom-built perfusion chamber on the stand of a Zeiss LSM 510 confocal microscope (Thornwood,

[2]The abbreviations used are: PKC, protein kinase C; PA-GFP, photo-activatable green fluorescent protein; NES, nuclear exclusion sequence; AVP, vasopressin; PDBu, phorbol 12,13-dibutyrate; BAPTA, 1,2-bis(2-aminophenoxy)ethane-*N*,*N*,*N*′,*N*′-tetraacetic acid; AM, acetoxymethyl; FRAP, fluorescence recovery after photobleaching; $InsP_3$, inositol 1,4,5-trisphosphate.

NY) as described previously (16,23,24). Cells were imaged using time-lapse confocal microscopy with a 63×,1.4 NA water-immersion objective lens. Cells transfected with PA-GFP were co-transfected with DsRed-NES to identify the transfected cells and to determine their nuclear boundary. Photo-activated GFP was excited at 488 nm and detected at 500–530 nm, while DsRed-NES was excited at 543 nm and detected at >560 nm.

Two-photon Activation and Calcium Uncaging

PA-GFP was activated by two-photon excitation using a mode-locked femptosecond-pulsed Coherent Chameleon Ti:Sapphire laser (Santa Clara, CA) tuned to 800 nm. For photo-release of Ca^{2+} from DM-nitrophen, the laser was tuned to 730 nm (19,25,26). In all cases a Zeiss LSM 510 confocal microscope was used for imaging.

Fluorescence Recovery after Photobleaching (FRAP)

Using the same confocal microscope, a 4-μm^2 area of the nucleus or cytosol of cells transfected with pEGFP C2 was photobleached using the 488 nm line of an argon laser, then fluorescence recovery was monitored by time-lapse confocal microscopy (5). Bleaching was sufficient to eliminate ~80% of the fluorescence in the region of interest.

Calcium Imaging

Fura Red was used for Ca^{2+} imaging to minimize spectral overlap with GFP. PA-GFP was activated in the cytosol of cells using two-photon excitation as described above. Cells were incubated for 30 min at 37 °C with Fura Red/AM (6 μ_M) and then incubated for a further 10 min at room temperature with DM-nitrophen/AM (1 μ_M). Cells were excited at 488 nm and observed simultaneously at 500–530 and >620 nm to detect PA-GFP and Fura Red emission signals, respectively. Once base-line fluorescence had been determined, Ca^{2+} was uncaged in a 1.4-μm^2 perinuclear region using two-photon excitation.

Statistics

PA-GFP fluorescence is represented as a percentage of the fluorescence detected at the time of activation. Values are the average obtained over a 10-s interval collected at least 120 s after activation. Fura Red fluorescence is represented as the percentage decrease in fluorescence from base line. Data are represented as mean ± S.E. Means between groups were compared using Student's *t* test, and $p < 0.05$ was taken to indicate statistically significant differences.

RESULTS

GFP Does Not Freely Cross the Nuclear Envelope

SKHep1 cells were transfected with PA-GFP, along with DsRed-NES as a marker of successful transfection and to serve as an indicator of the nuclear boundary. Cells were monitored by confocal microscopy as two-photon excitation was used to locally activate fluorescence of PA-GFP in specific subcellular regions. PA-GFP was activated either in the cytosol of individual cells, as determined by the presence of DsRed fluorescence (Fig. 1, *A* and *B*), or in the nucleus, as determined by the absence of DsRed (Fig. 1*C*). Fluorescence activated in a 4-μm^2 region within the cytosol spread throughout the remainder of the cytosol within 10 s but did not enter the nucleus, even after 4 min ($n = 8$ cells; Fig. 1*D*). Similarly, fluorescence activated in a 4-μm^2 region within the nucleus spread throughout the remainder of the nucleus within 10 s but did not enter the cytosol, even after 4 min ($n = 8$ cells; Fig. 1*E*). This indicates that the nuclear membrane represents a bidirectional barrier to the diffusion of the 27-kDa GFP molecule.

FRAP has previously been used to monitor movement of molecules smaller than 40 kDa in size, including GFP, across the nuclear membrane (5,27). In contrast to the above findings,

such studies had suggested that GFP freely diffuses across the nuclear envelope. To understand the basis for this apparent discrepancy, FRAP experiments previously reported by others (5) were replicated in SKHep1 cells. Cells were co-transfected with eGFP and DsRed-NES, then monitored by confocal microscopy as GFP fluorescence was photobleached in 15-μm^2 regions within either the cytosol (n = 4 cells) or nucleus (n = 4 cells) using the 30 milliwatt argon laser of the confocal microscope. Fluorescence in the photobleached region recovered to a similar extent regardless of the cellular compartment in which the GFP was bleached (Fig. 2), similar to what has been reported in other cell systems (5).

Since the confocal FRAP method delivers more power than two-photon excitation to the cell and does so in multiple focal planes rather than in a single plane of focus (28,29), the findings suggest that measurements of transport across the nuclear boundary using FRAP may have been influenced in part by phototoxic effects. To investigate this, we reasoned that the energy introduced through FRAP could lead to oxidation and free radical formation, which in turn would hypersensitize the inositol 1,4,5-trisphosphate ($InsP_3$) receptors (30,31) and increase intracellular Ca^{2+}. To test this, FRAP experiments were repeated in the presence of the cell-permeant reducing agent dithiothreitol (100 μM) or the cell-permeant Ca^{2+} chelator BAPTA-AM (30 μM). In the presence of either compound, GFP fluorescence recovery was blocked or attenuated (n = 4 experiments under each condition; Fig. 3). These findings provide evidence that the permeability of the nuclear envelope to GFP observed using FRAP is due in part to phototoxic effects of this measurement technique.

AVP Increases the Permeability of the Nuclear Envelope

SKHep1 cells expressing DsRed-NES and PA-GFP were monitored during perfusion with AVP (1 μM). PA-GFP then was activated in the cytosol or nucleus within 60 s of AVP stimulation. In contrast to what was observed in control (unstimulated) cells, fluorescence activated in the cytosol spread throughout these cells, including into the nucleus (n = 8 cells; Fig. 4, *A* and *B*). A brief delay of less than 5 s was observed at the nuclear envelope, which may reflect the reduced cross-sectional area available for diffusion of GFP relative to the cytosol. The vasopressin receptor antagonist [deamino-pen^1, *O*-Me-Tyr^2, Arg^8)]vasopressin (10 μM) blocked this action (n = 6 cells), demonstrating that it is a specific effect of AVP stimulating the V_{1a} receptor (Fig. 4*B*). Unlike what was observed during cytosolic photoactivation, but similar to what was observed in unstimulated cells, fluorescence activated in the nucleus was contained within that compartment during stimulation with AVP (n = 8 cells; Fig. 4, *C* and *D*). This indicates that AVP rapidly increases nuclear permeability to GFP but in a unidirectional fashion from cytosol to nucleus.

Activation of Other G Protein-coupled Receptors Increases Nuclear Permeability in a Manner Similar to That of AVP

The effects of various other agonists on nuclear permeability were tested to investigate whether the actions of AVP reflect a general effect of stimulating receptors that couple to G_q. Cells were stimulated with angiotensin (100 μM) to stimulate the AT receptor, phenylephrine (100 μM) to stimulate the α_{1B} adrenergic receptor, or ATP (100 μM) to stimulate the P2Y nucleotide receptor. PA-GFP activated in the cytosol after perifusion with either angiotensin (n = 7 cells), phenylephrine (n = 7 cells), or ATP (n = 8 cells) was visible throughout the cell (Fig. 5, *A*–*C*). These effects also appear to be specific to the angiotensin, α_{1B}-adrenergic, and P2Y nucleotide receptors, as they were blocked by [Sar^1, Val^5, Ala^8] antiotensin II acetate (100 μM), prazosin (100 μM), or suramin (100 μM), respectively (n = 4–6 cells; Fig. 5, A–C). As was seen in both unstimulated and AVP-stimulated cells, PA-GFP activated in the nucleus during stimulation with angiotensin, phenylephrine, or ATP did not move across the nuclear envelope. These findings suggest that the rapid unidirectional increase in nuclear permeability is a general effect of stimulation of this class of G protein-coupled receptors.

The Effect of AVP on Nuclear Permeability Is Mediated by Cytosolic Ca^{2+}

Binding of AVP to the vasopressin V_{1a} receptor leads to formation of $InsP_2$ and diacylglycerol, which in turn increases cytosolic Ca^{2+} and activates PKC, respectively (10,32). To determine the mechanism by which AVP affects nuclear permeability, the contribution of each of these second messengers was investigated.

Cytosolic Ca^{2+} was increased in a receptor-independent fashion using the SERCA pump inhibitor thapsigargin (2 μ_M). PA-GFP then was activated in the cytosol or nucleus within 60 s of treatment. After activation in the cytosol PA-GFP spread throughout the cell (n = 8 cells; Fig. 6*A*). In contrast, fluorescence activated in the nucleus was contained (n = 8 cells; data not shown). Thus increasing cytosolic Ca^{2+} using thapsigargin mimics the effect of AVP on nuclear permeability, suggesting that an increase in cytosolic Ca^{2+} is sufficient to increase nuclear permeability. In separate experiments, cells were loaded with the low affinity Ca^{2+} dye magfluo-4 to monitor the effects of thapsigargin on Ca^{2+} stores. These studies revealed that thapsigargin induced a 43 ± decrease in magfluo-4 fluorescence within the nuclear envelope (Fig. 6, *B* and *C*), so that the increase in nuclear perme-ability occurs despite a concomitant decrease in nuclear envelope Ca^{2+} stores. To investigate whether the increase in cytosolic Ca^{2+} is not only sufficient but necessary as well, cells were pretreated with the cell-permeant Ca^{2+} chelator BAPTA/AM (30 μ_M) before perfusion with AVP. When PA-GFP was activated in either the cytosol or nucleus under these conditions, fluorescence did not spread between the two subcellular compartments (n = 8 cells; Fig. 6*D*). These findings provide evidence that increases in cytosolic Ca^{2+} are both necessary and sufficient for the effect of AVP on nuclear permeability.

As an additional way to investigate the effects of cytosolic Ca^{2+} on nuclear permeability, small amounts of caged Ca^{2+} were photoreleased in regions of the cytoplasm near the nuclear envelope (Fig. 7). For these studies, cells were transfected with PA-GFP plus DsRed-NES as before and then were loaded with the cell-permeant Ca^{2+} cage DM-nitrophen/AM and the long wavelength Ca^{2+} dye Fura Red/AM. For these experiments PA-GFP was activated at 860 nm rather than 800 nm to avoid premature release of caged Ca^{2+}. Two-photon activation of GFP at 860 nm in a discrete region of cytosol (Fig. 7*A*) resulted in GFP fluorescence that spread throughout cytosol but not into the nucleus. Subsequently, two-photon excitation at 730 nm was used to photorelease caged Ca^{2+} in a small region near the nuclear envelope (Fig. 7*A*). This resulted in a transient, localized perinuclear increase in Ca^{2+}, as confirmed by a transient decrease in Fura Red fluorescence detected in the same region (Fig. 7*B*). GFP fluorescence appeared in the nucleus within 0.5 s of the perinuclear increase in cytosolic Ca^{2+}. Intranuclear GFP fluorescence was observed initially in the region of the nucleus nearest the increase in cytosolic Ca^{2+} and then spread throughout the nucleus (n = 3 cells; Fig. 7*C*). This provides direct evidence that local, perinuclear increases in cytosolic Ca^{2+} result in increased permeability of the nuclear envelope.

The Effect of AVP on Nuclear Permeability Is Partially Mediated by PKC

PKC was increased in a receptor-independent fashion using PDBu. PA-GFP then was activated in the cytosol or nucleus within 60 s of treatment. Fluorescence from PA-GFP activated in the cytosol (n = 8 cells; Fig. 8*A*) or nucleus (n = 8 cells; data not shown) under these conditions did not cross the nuclear envelope. Thus activating PKC does not mimic the effect of AVP on nuclear permeability. To investigate whether PKC plays a contributing role to the effects of AVP, cells were pretreated with the cell-permeant myristolated PKC inhibitor (100 μ_M) before perfusion with AVP. Fluorescence from PAG-FP activated in the cytosol spread throughout these cells, including into the nucleus, although it did not reach equilibrium as in the case of AVP alone (n = 8 cells; Fig. 8*B*). Fluorescence activated in the nucleus did not spread to the

cytosol ($n = 8$ cells; data not shown). Together, these findings provide evidence that PKC plays only a limited role in the effect of AVP on nuclear permeability.

DISCUSSION

Here we report that cytosolic Ca^{2+} regulates permeability of the nuclear envelope. A 27-kDa photo-activatable green fluorescent protein (22) was used to monitor nuclear permeability, and this protein was found to be restricted in its movement across the nuclear envelope. Initially PA-GFP is distributed throughout the cell as is evidenced by the fact that it can be activated in the nucleus or cytosol. It is unclear how or when PA-GFP equilibrates across the nuclear envelope in light of our findings, but possibilities include that this occurs when the nuclear envelope breaks down during mitosis or else as a result of periodic stimulation by growth factors in the culture medium. When PA-GFP was activated in the cytosol it spread throughout that compartment but did not move into the nucleus, whereas activated PA-GFP in the nucleus did not spread into the cytosol. These findings demonstrate that a protein of 27 kDa does not freely cross the nuclear envelope in unstimulated cells, which in turn suggests that the nuclear envelope is more selective in terms of the size of molecules which can freely diffuse across it than was previous considered. Previous reports instead suggested that GFP (5) as well as larger, 40-kDa fluorescent dextrans (6) freely cross the nuclear envelope. The previous GFP study used FRAP to examine transfer of the fluorescent protein between cytosol and nucleus (5), and our findings confirm that GFP readily crosses the nuclear envelope when redistribution is monitored by the FRAP technique. What accounts for this apparent discrepancy? The FRAP technique uses one-photon excitation to bleach GFP, while PA-GFP was excited here using two-photon excitation. FRAP delivers more energy than two-photon excitation to the cell and does so throughout the light path rather than merely at the focal point (28,29). These considerations suggest that cellular photodamage due to the FRAP technique could be responsible for alterations in nuclear permeability. This was supported by our observation that GFP movement between nucleus and cytosol after photobleaching is inhibited by reducing agents or Ca^{2+} chelators. These findings are consistent with the fact that single photon laser light can induce oxidation and free radical formation and that oxidation of the $InsP_3$ receptor increases its sensitivity and facilitates Ca^{2+} release (30,31). Microinjection or electroporation of fluorescent dextrans in the size range of GFP would not render cells susceptible to photodamage, yet these approaches also led to the observation that such compounds permeate the nuclear envelope (6). However, the mechanical stress of these techniques has been associated with release of ATP, and subsequent autocrine stimulation of P2Y receptors (33, 34). We found here that stimulation of P2Y receptors itself is sufficient to increase nuclear permeability, so that one may not be able to draw conclusions about nuclear pore permeability from studies in which fluorescent labels are introduced into the cell by microinjection or electroporation. Therefore, two-photon photoactivation of a fluorescent probe in specific subcellular regions has provided a way to make novel assessments of the short term regulation of nuclear pore permeability.

A major finding of this study is that G_q protein-coupled hormones increase the permeability of the nuclear envelope to PAGFP. Activation of four different types of plasma membrane receptors produced this effect, suggesting that it was due to one or more of their common second messengers, rather than resulting from an effect of activation of one specific type of hormone receptor. Receptor-independent increases in Ca^{2+} but not PKC could duplicate this effect, and it be blocked by buffering cytosolic Ca^{2+} but not by inhibiting activation of PKC. Together, these observations suggest that the increase in Ca^{2+} was specifically responsible for increasing the permeability of the nuclear envelope. Local elevations in Ca^{2+} along a discrete portion of the nuclear envelope, induced by perinuclear flash photolysis of caged Ca^{2+}, resulted in local increases in nuclear permeability, which provides direct confirmatory evidence that Ca^{2+} mediates this increase in permeability. The Ca^{2+} cage used here can bind to and release

Mg^{2+} (35), but we measured cytosolic Ca^{2+} directly to confirm that two-photon flash photolysis of DM-nitrophen results in a localized increase in Ca^{2+} under the conditions used here. It is unclear how cytosolic Ca^{2+} modulates nuclear pore permeability. The unidirectional nature of the effect suggests this may occur by regulated diffusion. This in turn could be a result of the membrane potential differences that can occur in a subcellular pattern across biological membranes (36) or else may reflect osmotic conditions in the nucleus, which have been characterized only partially to date (37). The nuclear pore protein gp210 contains an EF-hand Ca^{2+} binding domain that could serve as a cytosolic Ca^{2+} sensor (38), but it is thought that this protein instead senses whether Ca^{2+} stores within the nuclear envelope are filled (39). There is also evidence that calmodulin can regulate gating of the nuclear pores, but calmodulin must be overexpressed to do so, and even calmodulin mutants that cannot bind to Ca^{2+} will increase nuclear pore permeability (21). A collection of studies together suggest that depletion of Ca^{2+} within the nuclear envelope leads to a conformational change in the nuclear pore that results in its blockage by the nuclear plug that resides within the lumen of the pore (7-9,39). However, here we observed an increase in nuclear pore permeability even in cells treated with thapsigargin, which reduces Ca^{2+} stores in the endoplasmic reticulum and nuclear envelope (16). We also observed that four different agents that increase cytosolic Ca^{2+} via $InsP_3$ each increase nuclear permeability as well, even though $InsP_3$ acts via $InsP_3$ receptors to decrease permeability of nuclear pores in isolated nuclei (9). Therefore the effect of cytosolic Ca^{2+} on nuclear permeability that we observed is independent of effects that may result from depletion of Ca^{2+} from the nuclear envelope.

Several biological agents have been identified that modulate permeability of the nuclear pore. Infection of cells with polio-virus causes structural changes in the nuclear pore complex, and these are associated with functional changes as well. Influx of GFP into the nucleus is increased in infected cells, and cells also lose the ability to retain NLS-tagged GFP within the nucleus (40). Both glucocorticoids (41) and mineralocorticiods (42) rapidly and transiently increase the permeability of the nuclear pore to dextrans in the 10–20-kDa size range. This action precedes the initiation of gene transcription that is induced by these steroid hormones and thus may play a role in mediating that effect (40,41). Here we found that vasopressin, angiotensin, phenylephrine, and ATP each increase nuclear permeability. Each of these agents can stimulate gene transcription and cell growth as well (43-46). The way in which these effects are mediated has not been established, but previous findings suggest several possible mechanisms. Both vasopressin and ATP increase free Ca^{2+} within the nucleus (47,48), and nuclear Ca^{2+} can stimulate gene transcription through several pathways (11,12,49). In addition, ATP, AVP, and angiotensin each activate mitogen-activated protein kinases (46,50,51). By showing that agents that elevate cytosolic Ca^{2+} allow the influx of 27 kDa proteins from cytosol reveals the possibility that Ca^{2+} agonists may also initiate gene transcription by permitting transcription factors or other proteins to enter the nucleus. Further work will be needed to verify this putative role of Ca^{2+} agonists, as well as to determine the target of Ca^{2+} in the nuclear pore complex, and to understand why the change in permeability induced by cytosolic Ca^{2+} is unidirectional.

REFERENCES

1. Ohno M, Fornerod M, Mattaj IW. Cell 1998;92:327–336. [PubMed: 9476893]
2. Rout MP, Aitchison JD. J. Biol. Chem 2001;276:16593–16596. [PubMed: 11283009]
3. Akey CW. J. Cell Biol 1989;109:955–970. [PubMed: 2768344]
4. Pante N, Kann M. Mol. Biol. Cell 2002;13:425–434. [PubMed: 11854401]
5. Wei X, Henke VG, Strubing C, Brown EB, Clapham DE. Biophys. J 2003;84:1317–1327. [PubMed: 12547812]
6. Thorogate R, Török K. J. Cell Sci 2004;117:5923–5936. [PubMed: 15522886]
7. Stehno-Bittel L, Perez-Terzic C, Clapham DE. Science 1995;270:1835–1838. [PubMed: 8525380]

8. Greber UF, Gerace L. J. Cell Biol 1995;128:5–14. [PubMed: 7822421]
9. Moore-Nichols D, Arnott A, Dunn RC. Biophys. J 2002;83:1421–1428. [PubMed: 12202368]
10. Berridge MJ, Bootman MD, Roderick HL. Nat. Rev. Mol. Cell. Biol 2003;4:517–529. [PubMed: 12838335]
11. Hardingham GE, Chawla S, Johnson CM, Bading H. Nature 1997;385:260–265. [PubMed: 9000075]
12. Pusl T, Wu JJ, Zimmerman TL, Zhang L, Ehrlich BE, Berchtold MW, Hoek JB, Karpen SJ, Nathanson MH, Bennett AM. J. Biol. Chem 2002;277:27517–27527. [PubMed: 11971908]
13. Llinas R, Sugimori M, Silver RB. Science 1992;256:677–679. [PubMed: 1350109]
14. Fernandez-Chacon R, Konigstorfer A, Gerber SH, Garcia J, Matos MF, Stevens CF, Brose N, Rizo J, Rosenmund C, Sudhof TC. Nature 2001;410:41–49. [PubMed: 11242035]
15. Ito K, Miyashita Y, Kasai H. EMBO J 1997;16:242–251. [PubMed: 9029145]
16. Minagawa N, Kruglov EA, Dranoff JA, Robert ME, Gores GJ, Nathanson MH. J. Biol. Chem 2005;280:33637–33644. [PubMed: 16027162]
17. Craske ML, Fivaz M, Batada NN, Meyer T. J. Cell Biol 2005;170:1147–1158. [PubMed: 16186260]
18. Oancea E, Meyer T. Cell 1998;95:307–318. [PubMed: 9814702]
19. Echevarria W, Leite MF, Guerra MT, Zipfel WR, Nathanson MH. Nat. Cell Biol 2003;5:440–446. [PubMed: 12717445]
20. Dyachok O, Isakov Y, Sagetorp J, Tengholm A. Nature 2006;439:349–352. [PubMed: 16421574]
21. Thorogate R, Török K. Calcium Binding Proteins 2006;1:36–44.
22. Patterson GH, Lippincott-Schwartz J. Science 2002;297:1873–1877. [PubMed: 12228718]
23. Hagar RE, Burgstahler AD, Nathanson MH, Ehrlich BE. Nature 1998;396:81–84. [PubMed: 9817204]
24. Hirata K, Nathanson MH, Sears ML. Proc. Natl. Acad. Sci. U. S. A 1998;95:8381–8386. [PubMed: 9653195]
25. Brown EB, Shear JB, Adams SR, Tsien RY, Webb WW. Biophys. J 1999;76:489–499. [PubMed: 9876162]
26. Leite MF, Burgstahler AD, Nathanson MH. Gastroenterology 2002;122:415–427. [PubMed: 11832456]
27. Howell JL, Truant R. BioTechniques 2002;32:80–82, 84, 86, 87. [PubMed: 11808703]
28. Denk W, Strickler JH, Webb WW. Science 1990;248:73–76. [PubMed: 2321027]
29. Potter SM. Curr. Biol 1996;6:1595–1598. [PubMed: 8994823]
30. Bootman MD, Taylor CW, Berridge MJ. J. Biol. Chem 1992;267:25113–25119. [PubMed: 1334081]
31. Rooney TA, Renard DC, Sass EJ, Thomas AP. J. Biol. Chem 1991;266:12272–12282. [PubMed: 2061312]
32. Morel A, O'Carroll AM, Brownstein MJ, Lolait SJ. Nature 1992;356:523–526. [PubMed: 1560825]
33. Osipchuk Y, Cahalan M. Nature 1992;359:241–244. [PubMed: 1388246]
34. Schlosser SF, Burgstahler AD, Nathanson MH. Proc. Natl. Acad. Sci. U. S. A 1996;93:9948–9953. [PubMed: 8790437]
35. Kaplan JH, Ellis-Davies GC. Proc. Natl. Acad. Sci. U. S. A 1988;85:6571–6575. [PubMed: 3137570]
36. Yeung T, Terebiznik M, Yu L, Silvius J, Abidi WM, Philips M, Levine T, Kapus A, Grinstein S. Science 2006;313:347–351. [PubMed: 16857939]
37. Phair RD, Misteli T. Nature 2000;404:604–609. [PubMed: 10766243]
38. Greber UF, Gerace L. J. Cell Biol 1992;116:15–30. [PubMed: 1370490]
39. Perez-Terzic C, Pyle J, Jaconi M, Stehno-Bittel L, Clapham DE. Science 1996;273:1875–1877. [PubMed: 8791595]
40. Belov GA, Lidsky PV, Mikitas OV, Egger D, Lukyanov KA, Bienz K, Agol VI. J. Virol 2004;78:10166–10177. [PubMed: 15331749]
41. Shahin V, Ludwig Y, Schafer C, Nikova D, Oberleithner H. J. Cell Sci 2005;118:2881–2889. [PubMed: 15976447]
42. Buchholz I, Enss K, Schafer C, Schlune A, Shahin V, Oberleithner H. J. Membr. Biol 2004;199:135–141. [PubMed: 15457370]

43. Nicou A, Serriere V, Prigent S, Boucherie S, Combettes L, Guillon G, Alonso G, Tordjmann T. FASEB J 2003;17:1901–1903. [PubMed: 14519667]

44. Brasier AR, Jamaluddin M, Han Y, Patterson C, Runge MS. Mol. Cell. Biochem 2000;212:155–169. [PubMed: 11108147]

45. Markou T, Hadzopoulou-Cladaras M, Lazou A. J. Mol. Cell. Cardiol 2004;37:1001–1011. [PubMed: 15522277]

46. Thevananther S, Sun H, Li D, Arjunan V, Awad SS, Wyllie S, Zimmerman TL, Goss JA, Karpen SJ. Hepatology 2004;39:393–402. [PubMed: 14767992]

47. Fox JL, Burgstahler AD, Nathanson MH. Biochem. J 1997;326:491–495. [PubMed: 9291123]

48. Leite MF, Thrower EC, Echevarria W, Koulen P, Hirata K, Bennett AM, Ehrlich BE, Nathanson MH. Proc. Natl. Acad. Sci. U. S. A 2003;100:2975–2980. [PubMed: 12606721]

49. Carrion AM, Link WA, Ledo F, Mellstrom B, Naranjo JR. Nature 1999;398:80–84. [PubMed: 10078534]

50. Ren XR, Reiter E, Ahn S, Kim J, Chen W, Lefkowitz RJ. Proc. Natl. Acad. Sci. U. S. A 2005;102:1448–1453. [PubMed: 15671180]

51. Shenoy SK, Lefkowitz RJ. Sci. STKE 2005;2005:cm14. [PubMed: 16304060]

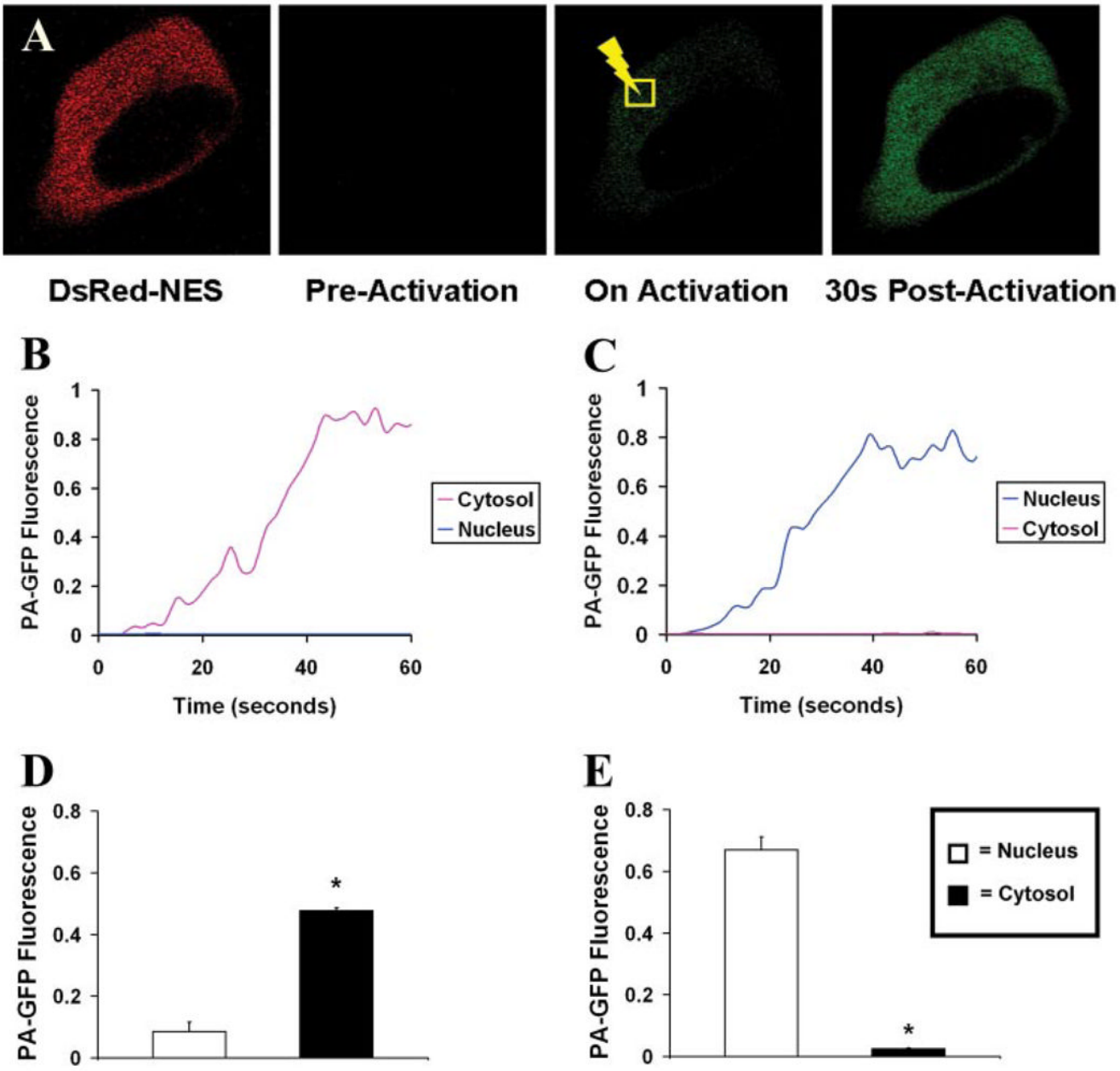

FIGURE 1. GFP fluorescence does not move freely between the nucleus and the cytosol

A, SKHep1 cells were transfected with PA-GFP, along with DsRed-NES as a cytosolic marker of transfection. PA-GFP was selectively activated in a small region (*yellow square*) within the cytosol (shown) or the nucleus (images not shown) of individual cells using two-photon excitation. GFP movement from that region was monitored over time and then represented graphically. *B*, GFP activated in a region within the cytosol spreads throughout the remainder of the cytosol but does not enter the nucleus, whereas GFP activated in a region within the nucleus spreads throughout the remainder of the nucleus but does not enter the cytosol (*C*). In both cases, traces represent PA-GFP fluorescence levels in the cytosol and nucleus distant from the point of activation. The *bar graph* summary shows that cytosolic fluorescence does not spread into the nucleus (n = 10 cells) (*D*), while nuclear fluorescence does not spread into the cytosol (n = 10 cells) (*E*). All cells were observed for at least 5 min after photoactivation of

GFP. In this and subsequent figures, fluorescence in each region within the cell is normalized relative to fluorescence in the region of activation immediately after two-photon excitation, which is set equal to one All values are mean ± S.E. (*, $p < 0.05$).

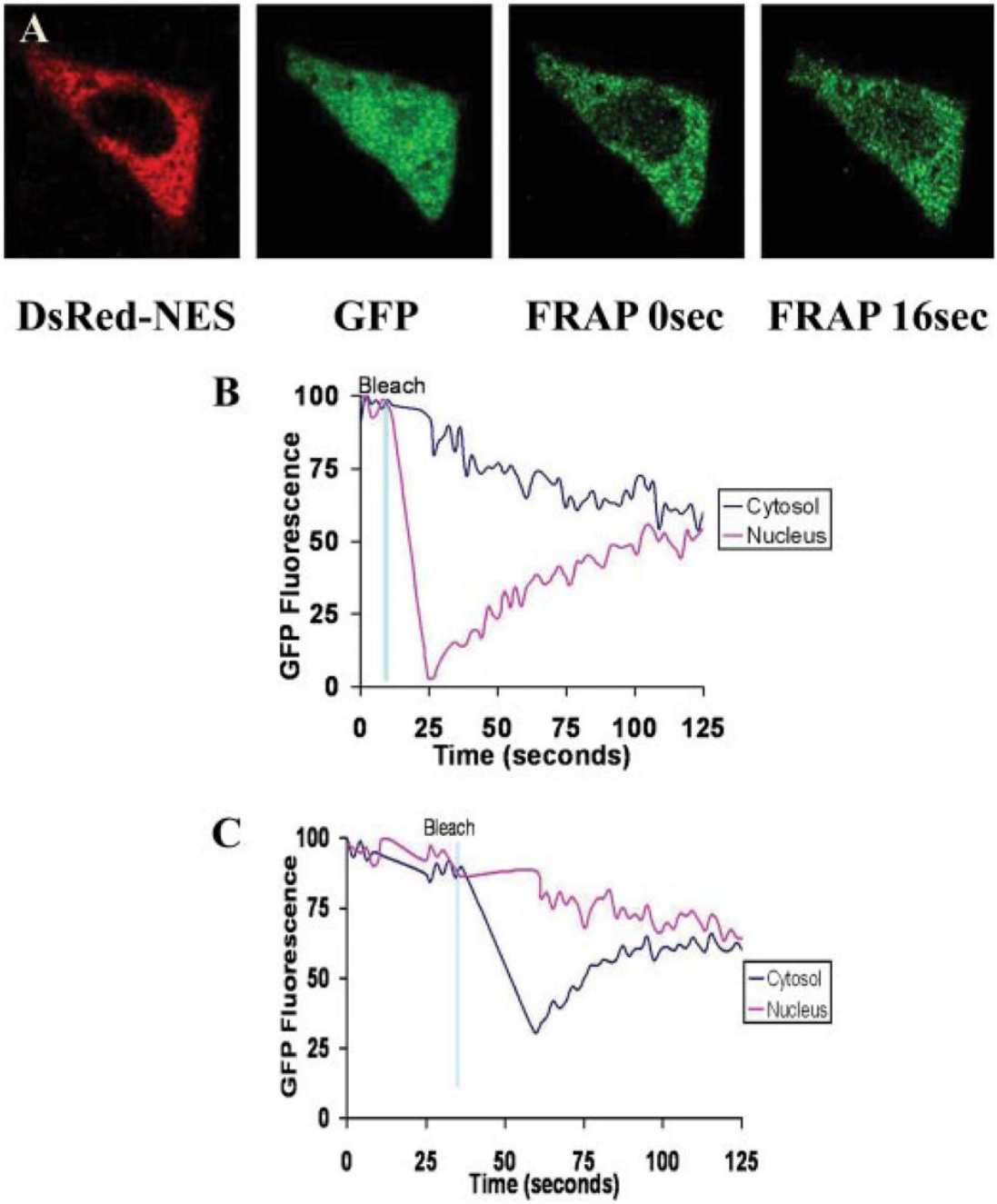

FIGURE 2. Nuclear permeability to GFP is altered by fluorescence recovery after photobleaching

A, serial confocal images demonstrate that GFP fluorescence recovers after photobleaching in the nucleus. Similar results were observed on photobleaching in the cytosol (data not shown). Photobleaching in either compartment was sufficient to eliminate ~50% of fluorescence in that compartment. Graphical representation illustrates that fluorescence moves from cytosol to nucleus (*B*) or from nucleus to cytosol (*C*) until GFP fluorescence re-equilibrates throughout the cell. Results are typical of what was observed in four cells in which cytosolic GFP was photobleached and four cells in which nuclear GFP was photobleached.

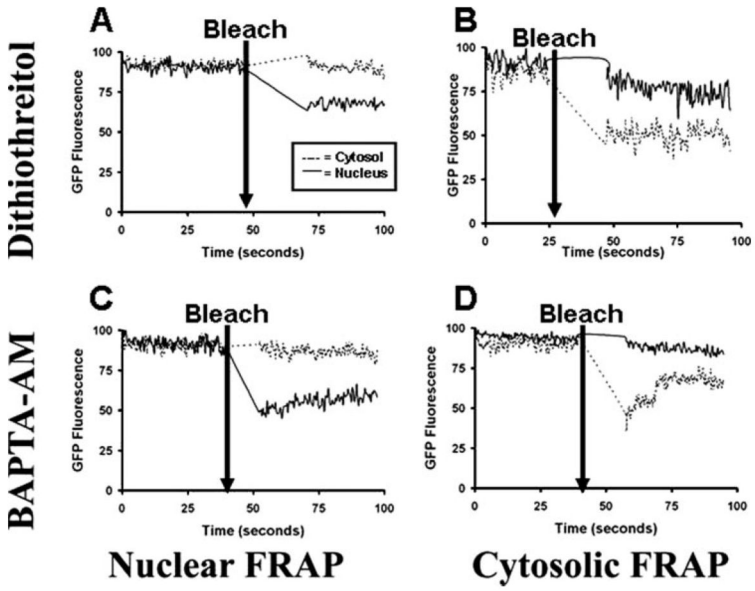

FIGURE 3. GFP fluorescence recovery after photobleaching is inhibited by either dithiothreitol or BAPTAAM

GFP FRAP across the nuclear membrane is reduced or blocked by the reducing agent and free radical scavenger dithiothreitol (*top panels*) or the Ca^{2+} chelator BAPTA-AM (*bottom panels*). SkHep1 cells were pre-incubated with dithiothreitol (100 μM; $n = 4$ cells) or BAPTA-AM (30 μM; $n = 4$ cells). Under each condition GFP was photobleached either within the nucleus (*left panels*) or cytosol (*right panels*), and the fluorescence recovery was observed. Each tracing is representative of what was observed in four separate cells and is normalized to the initial fluorescence within each compartment.

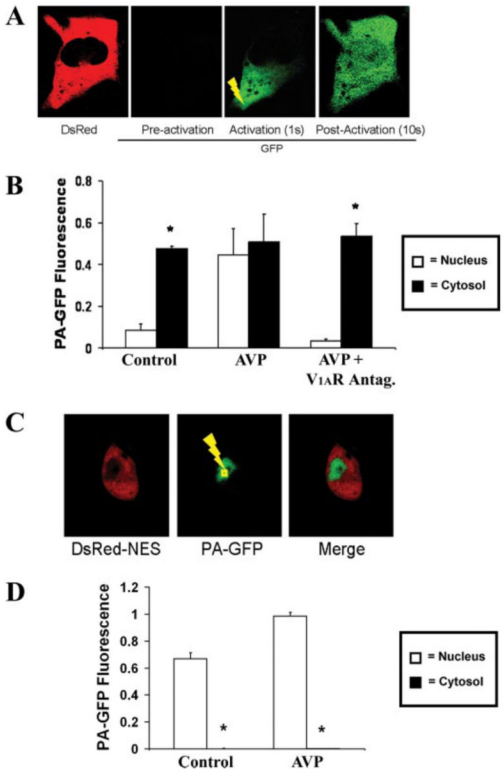

FIGURE 4. GFP moves from cytosol to nucleus in cells stimulated with AVP

Cells were perifused with AVP (1 μ_M), then PA-GFP was activated in the cytosol (*yellow lightning bolt*), and fluorescence was monitored throughout the cell. *A*, GFP fluorescence at the tip of the cell cytosol spreads throughout the cell, including into the nucleus. *B*, *bar graph* summary shows that, in contrast to controls, there is no significant difference ($p > 0.05$) between cytosolic and nuclear fluorescence in cells stimulated with AVP ($n = 6$ cells). The vasopressin receptor antagonist [deamino-pen^1,*O*-Me-Tyr^2,Arg^8]vasopressin eliminates the effect of AVP on nuclear permeability to GFP ($n = 6$ cells; *, $p < 0.05$). *C*, GFP fluorescence does not spread from nucleus to cytosol in the presence of AVP. *D*, *bar graph* summary shows that nuclear GFP fluorescence is significantly greater than cytosolic fluorescence (*, $p < 0.005$) in cells stimulated with AVP ($n = 6$ cells).

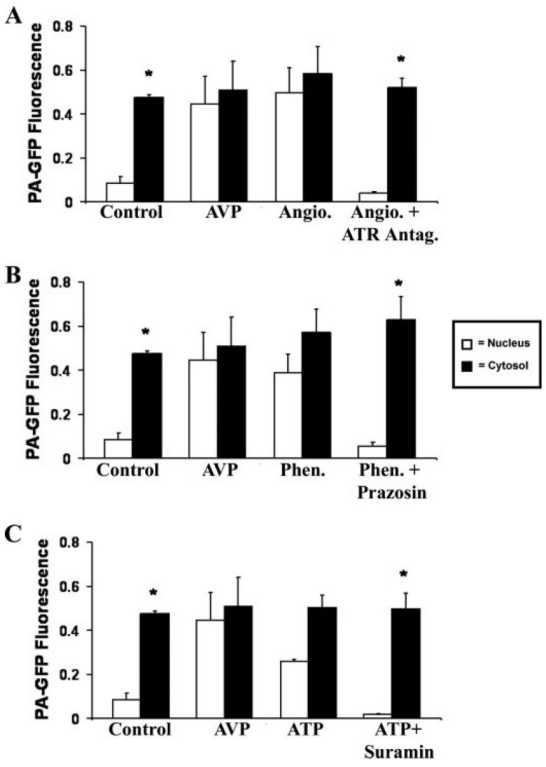

FIGURE 5. Angiotensin (*Angio.*), phenylephrine (*Phen.*), and ATP mimic the effect of AVP on nuclear permeability

Bar graph summaries show that there is no significant difference between cytosolic and nuclear fluorescence in cells stimulated with either angiotensin (100 μ_M; $n = 4$ cells) (*A*), phenylephrine (100 μ_M; $n = 6$ cells) (*B*), or ATP (100 μ_M; $n = 6$ cells) (*C*), followed by photoactivation of cytosolic PA-GFP. This effect is eliminated in the presence of antagonists for each plasma membrane receptor; the angiotensin receptor antagonist [Sar^1,Val^5,Ala^8]angiotensin II acetate (100 μ_M; $n = 6$ cells), the α-adrenergic receptor antagonist prazosin (100 μ_M; $n = 6$ cells), or the nucleotide receptor antagonist suramin (100 μ_M; $n = 4$ cells), respectively. This is similar to what is observed in cells stimulated with AVP but in contrast to what is observed in unstimulated cells (*, $p < 0.05$). GFP does not spread from nucleus to cytosol in cells stimulated with any of these three agonists (data not shown), similar to what was observed both in cells stimulated with AVP and in unstimulated cells.

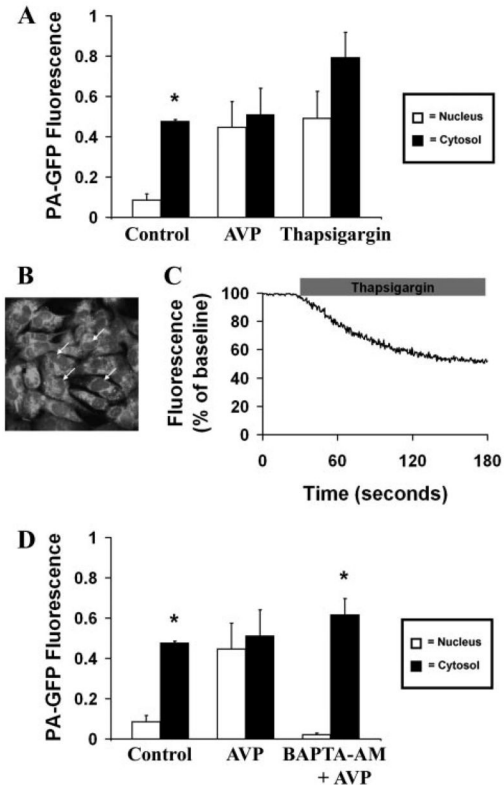

FIGURE 6. Increased cytosolic Ca^{2+} is necessary and sufficient to increase nuclear permeability

A, increased cytosolic Ca^{2+} is sufficient to increase nuclear permeability. The *bar graph* summary shows that there is no significant difference ($p < 0.05$) between cytosolic and nuclear fluorescence in cells stimulated with thapsigargin (2 μ_M; $n = 6$ cells), followed by photoactivation of cytosolic PA-GFP. This is similar to what is observed in cells stimulated with AVP but in contrast to what is observed in unstimulated cells. GFP does not spread from nucleus to cytosol in cells treated with thapsigargin (data not shown), similar to what was observed both in cells stimulated with AVP and in unstimulated cells. *B*, mag-fluo-4 labels Ca^{2+} stores, including in the nuclear envelope (*arrows*). *C*, thapsigargin decreases calcium stores. Cells were loaded with mag-fluo-4 and then treated with thapsigargin (2 μ_M). Thapsigargin induced a 43 ± 1% decrease in fluorescence in the nuclear envelope. Tracing is representative of what was observed in 30 separate cells. *D*, increased cytosolic Ca^{2+} is necessary to increase nuclear permeability. The *bar graph* summary shows that the effect of AVP (1 μ_M) on nuclear permeability is blocked (*, $p > 0.0005$) in cells pretreated with BAPTA/AM (30 μ_M; $n = 6$ cells), followed by photoactivation of cytosolic PA-GFP. GFP also does not spread from nucleus to cytosol in cells pretreated with BAPTA (data not shown), similar to what was observed both in cells stimulated with AVP and in unstimulated cells.

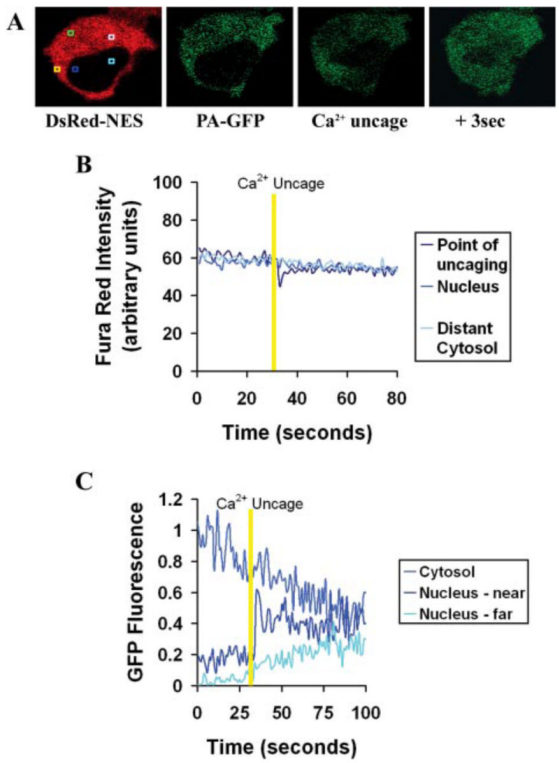

FIGURE 7. Perinuclear increases in Ca^{2+} locally increase the permeability of the nuclear envelope

A, serial confocal images show DsRed-NES fluorescence, the same cell after photoactivation of PA-GFP in the cytosol, and then photorelease of small amounts of Ca^{2+} near the nuclear envelope and then 3 s later. *Square regions* are as follows: point at which PA-GFP is activated (*green*), point at which Ca^{2+} is subsequently uncaged in cytosol (*yellow*), nearby region of nucleus (*blue*), distant region of nucleus (turquoise), distant region of cytosol (light blue). Fura Red and PA-GFP fluorescence were monitored at each point before, during, and after Ca^{2+} uncaging. *B*, graphical representation of Fura Red fluorescence in a separate cell shows that two-photon excitation of caged Ca^{2+} results in a highly transient and localized increase in cytosolic Ca^{2+} (downward deflection), which does not spread to elsewhere in the cytosol or the nucleus. *C*, graphical representation of cytosolic and nuclear fluorescence of GFP in the cell shown in *A* shows that GFP fluorescence appears in a localized portion of the nucleus following photorelease of Ca^{2+} in the cytosol near the nuclear envelope and that nuclear GFP fluorescence spreads from there to the rest of the nucleus. Results are representative of what was observed in three separate cells.

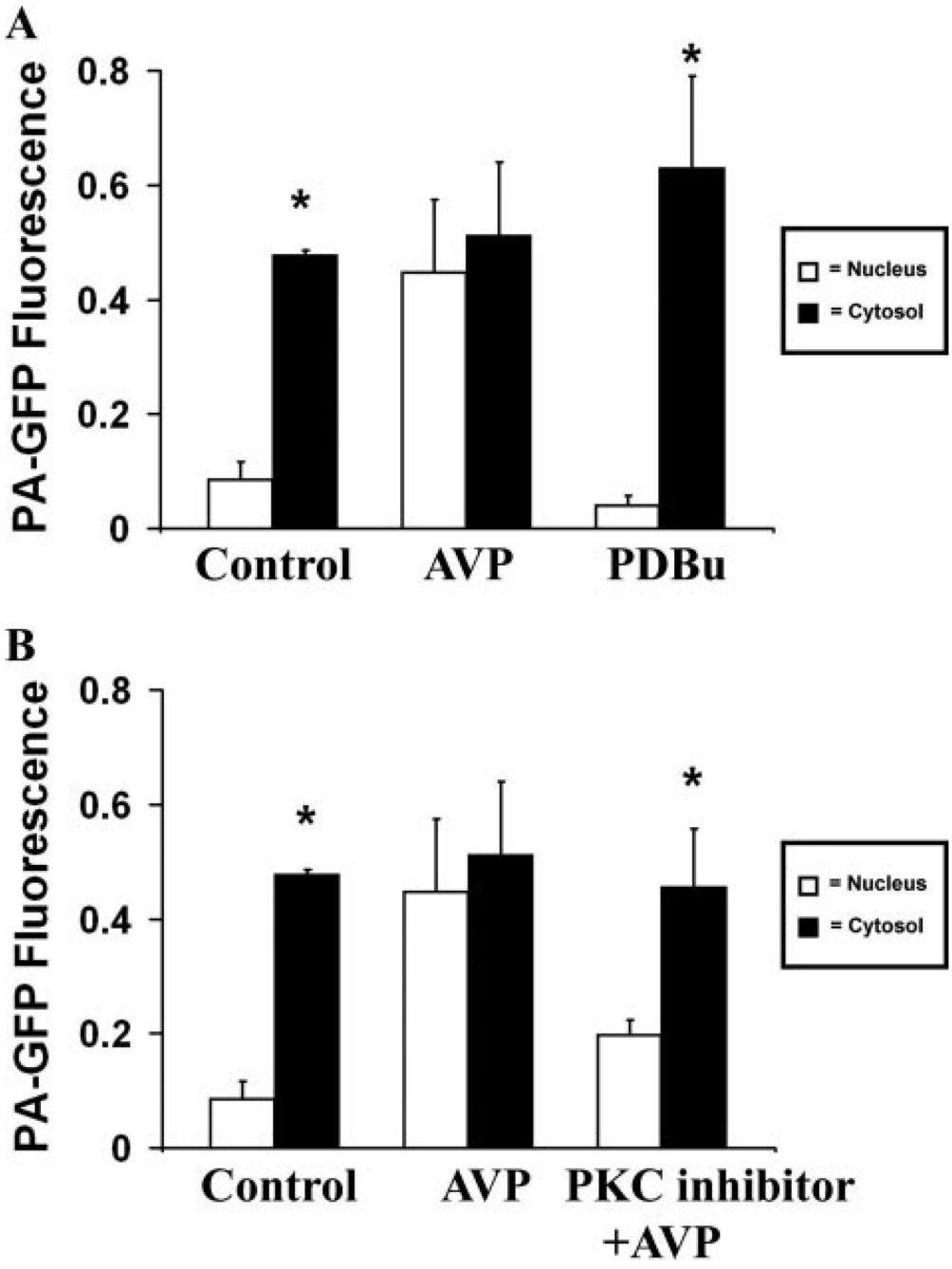

FIGURE 8. PKC activation is neither necessary nor sufficient to increase nuclear permeability

A, PKC activation is not sufficient to increase nuclear permeability. The *bar graph* summary shows that cytosolic GFP fluorescence remains higher than fluorescence within the nucleus (*, $p < 0.005$) in cells pretreated with PDBu (1 μ_M; $n = 6$ cells), followed by photoactivation of cytosolic PA-GFP. This is in contrast to what is observed in cells stimulated with AVP but similar to what is observed in unstimulated cells. GFP does not spread from nucleus to cytosol in cells treated with PDBu (data not shown), similar to what was observed both in cells stimulated with AVP and in unstimulated cells. *B*, PKC activation is not necessary to increase nuclear permeability and PKC inhibition partially reduces the effect of AVP on nuclear permeability. The *bar graph* summary shows that the effect of AVP (1 μ_M)on nuclear

permeability is not significantly reduced in cells pretreated with myristolated PKC inhibitor (100 μ_M; n = 6 cells), followed by photoactivation of cytosolic PA-GFP. GFP also does not spread from nucleus to cytosol in cells pretreated with this inhibitor (data not shown), similar to what was observed both in cells stimulated with AVP and in unstimulated cells.